Empirical Evaluation of Hexacopter Performance Post-Single Rotor Failure

L. Yan[1] and F. Ewere[2]
North Carolina State University, Raleigh, North Carolina, 27607, United States

Rotor failure is a potentially dangerous mode of failure in multirotors which may occur from structural or electrical damage. In scenarios where multirotors are used for urban air mobility, rotor failure may be catastrophic. Experimental in-situ observations of rotor failure and recovery were conducted using a subscale hexacopter. The hexacopter features a frame constructed primarily with carbon fiber and PLA plastic with a motor-to-motor diameter of 28 inches and six 12 x 4.5 inch propellers. Three clockwise and three counterclockwise rotors were positioned in a NPNPNP cross (X) configuration. Configured with a shutoff circuit for a single side rotor, constructed using an Arduino microcontroller and relay, gyroscope and accelerometer measurements for angular velocity and linear acceleration were collected using an inertial measurement unit (IMU) in a Pixhawk 6C flight controller. Normal operational flights as well as both clockwise and counter-clockwise side-rotor failure were both evaluated to observe the multirotor's deviance in pitch, yaw, and roll attitudes as well as the loss in T/W and available control authority index. Beginning with normal hovering flight, the hexacopter's shutoff circuit stops the delivery of power to one of the six rotors after a preprogrammed time delay. The hexacopter then corrects for the failed rotor and assumes a hovering configuration. IMU measurements are taken during the entire flight from power-on to power-off. Data on the performance of a hexacopter post-single rotor failure were collected and evaluated, showing an unstable yawing response to counterclockwise rotor failure and a successful recovery to clockwise rotor failure. Rotor failure caused a 16.68% decrease in the maximum T/W and a complete loss in control authority for the NPNPNP configuration hexacopter. Empirical observations showed that the hexacopter could recover back to a hovering state, but not a controllable state post-rotor failure, with a more severe yaw bias coming from counterclockwise rotor failure compared to clockwise rotor failure.

Nomenclature

T	=	thrust
T/W	=	thrust to weight ratio
x, y, z	=	translational axes
θ	=	pitch angle
φ	=	roll angle
ψ	=	yaw angle
W	=	weight
d	=	frame diameter
+, X	=	plus, cross configuration
f_i	=	thrust force from i^{th} rotor

Subscripts

max	=	maximum value
cg	=	center of gravity

[1]Undergraduate Student, Mechanical and Aerospace Engineering, Student Member
[2]Faculty Advisor | Associate Teaching Professor, Mechanical and Aerospace Engineering

I. Introduction

Multirotor aircraft are capable of vertical takeoff and landing (VTOL), and are a popular choice for applications in cargo transport and development for urban air mobility (UAM). Multirotors, and specifically hexacopters are a popular choice due to requiring less space to takeoff and land, with direct vertical motion being the greatest appeal [1]. As such, extensively evaluating the safety of a multirotor aircraft is vital, and requires safe responses to various failure modes [2]. One such example of a potentially devastating failure mode is single rotor failure. As multirotor aircraft rely entirely on the rotors for thrust and unlike fixed-wing aircraft, cannot glide, the safety of a multirotor in the event of rotor failure is essential to investigate [2]. Rotor failure may occur for a multitude of reasons including structural failure, as seen in Fig. 1, or power distribution errors. As such, the inclusion of redundant rotors is crucial for ensuring the safety of flight. The hexacopter provides the minimum number of rotors required to have redundancy in the event of rotor failure, and provides the best tradeoffs as discussed in Ref. [3] with a proper set of control laws.

Fig. 1 Rotor failure due to structure damage of hexacopter during test.

Previously performed simulations evaluated the recovery and response from a full-scale 1200 lb urban air mobility multirotor. During side rotor failure, the simulation results showed primarily a damped roll attitude response that fluctuated between -10 and 10 degrees post-rotor failure. Pitch attitude and yaw heading remained relatively unchanged [2]. Experimental evaluations of rotor failure have also previously been performed on subscale multirotors to evaluate their performance post-rotor failure which saw a small deviation in pitch and roll attitude responses but a more severe yaw response [4]. This study conducts an empirical evaluation of post-rotor failure on an NPNPNP cross (X) configuration hexacopter, evaluating the response and recovery ability of a 7-pound subscale hexacopter by observing the maximum deviation in pitch and roll attitudes as well as the yaw angle. Both the clockwise and counterclockwise side rotors were used in performing rotor failure tests.

II. Hexacopter Framework and Configuration

II A. Frame

The subscale hexacopter used in empirical evaluation consists of two main plates, six arms, and a landing gear. The main plate is composed of two carbon fiber plates with airborne hardware sandwiched between the two plates. Both plates are hexagonal in shape and have identical dimensions, with an edge-to-edge length of 12 inches. The two plates are held together using screws and nuts in between the arms. Figure 2 shows a top and rear view of the hexacopter.

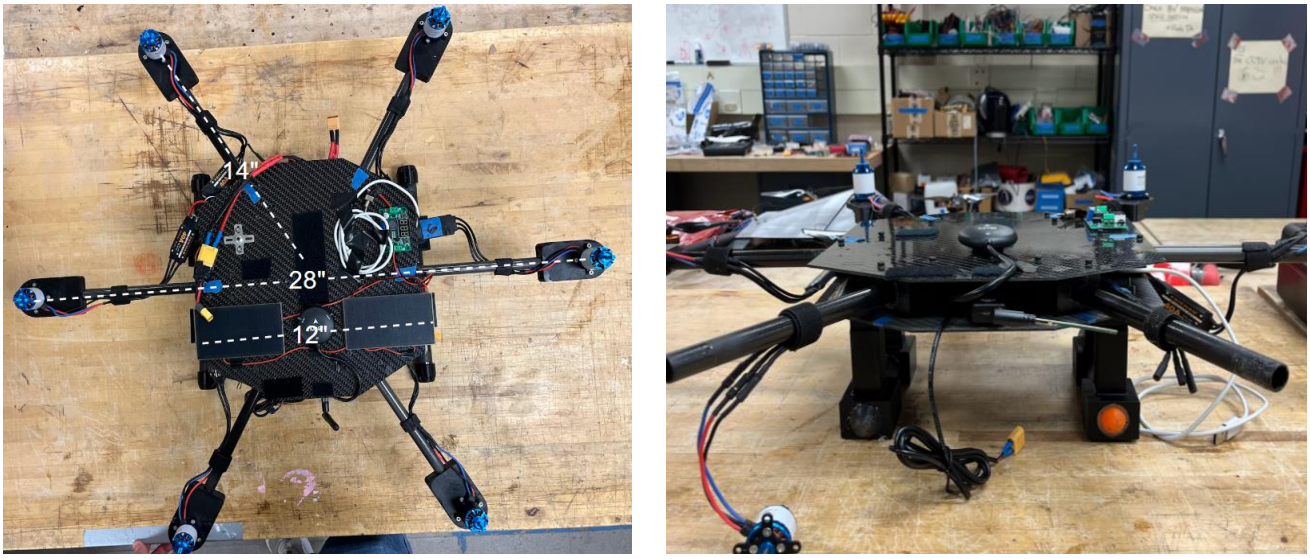

a) **b)**

Fig. 2 a) Top view and b) rear view of the hexacopter showing the main plate, arms, and landing gear.

Each arm consists of a carbon fiber tube with a diameter of 0.625 inches and has a fixture attached at either end that allows each arm to be connected to the main plate on one end, and to a motor on the other. Both fixtures are 3D printed with PLA plastic material. The total diameter of the hexacopter, measured center-to-center between two opposite motors, is 28 inches, with the center of each motor being placed 14 inches from the multirotor's center. The landing gear, as depicted in Fig. 2, is composed of a vertical segment that extends from the bottom plate of the hexacopter. Designed to only endure a compressional load, the landing gear transitions from vertical legs to a horizontal component made of a carbon tube attached to the legs via hot glue.

II B. Propulsion System

Six 980kV motors are utilized in the multirotor's propulsion system. Six propellers, three conventional and three pusher, accompany the motors. All six propellers have a tip-to-tip diameter of 12 inches and a pitch of 4.5 inches. The propellers are arranged in the NPNPNP cross (X) configuration [5] as seen in Fig. 3. Three rotors spin clockwise while three rotors spin counterclockwise. Connected to each motor is a 40A limit electronic speed controller (ESC). The ESCs control the rate that each motor spins at via pulse width modulation (PWM) signals from the flight controller that directly translate into the rotational speed of the motors. The ESCs also control the voltage of the circuit between the Li-Po battery power source and the motor, ensuring that the motor does not attempt to speed up too quickly and damage itself. A total of six ESCs are used, one connected to each motor on the hexacopter. All six ESCs meet at the central power distribution board (PDB) where they are soldered to the board's output terminals.

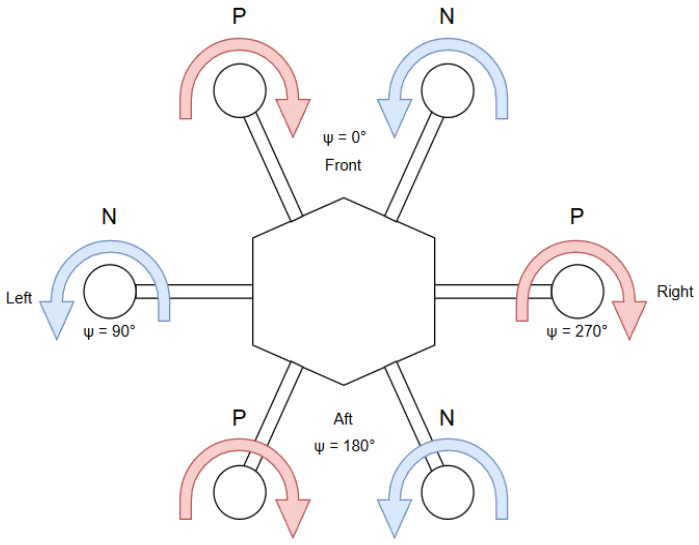

Fig. 3 Propeller rotation directions on NPNPNP-X configuration.

II C. Control Architecture

The main flight control computer used by the hexacopter is a Pixhawk 6C. The Pixhawk communicates over the PPM signal protocol to a FlySky FS-iA6B receiver that is binded to FlySky FS-i6X transmitter controlled by the

safety pilot. Additional hardware such as a GPS and radio antenna are connected to the Pixhawk 6C which provides the flight controller with telemetry data that later is transmitted to the ground station. Using pulse width modulation (PWM), the Pixhawk communicates with the electronic speed controllers (ESCs) for all six motors simultaneously. Based on the stick movements from the transmitter or from the flight controller's stability and control algorithm, the rotational speed of the motors are controlled in order to keep the hexacopter level in operational and post-rotor failure flight. Figure 4 depicts a block diagram which shows an overview of the communication system built into the hexacopter.

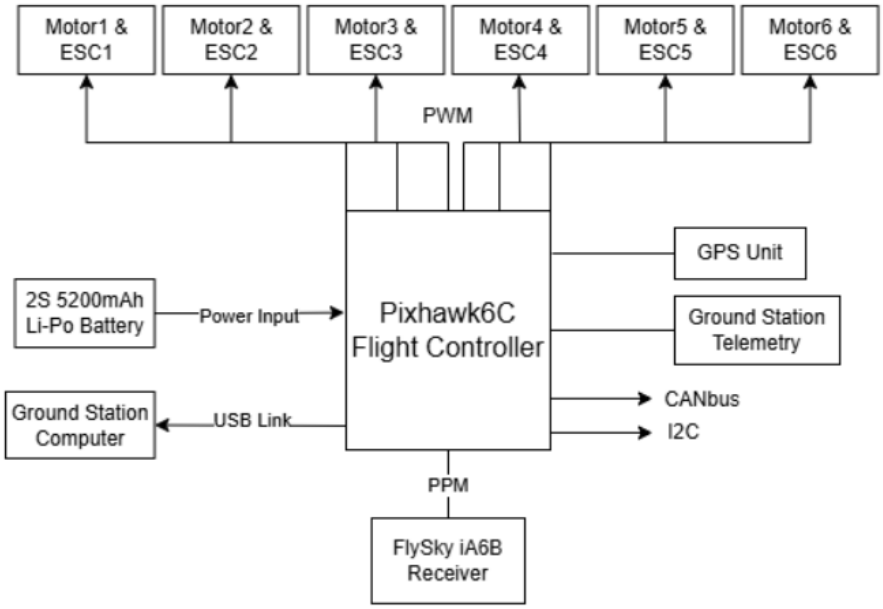

Fig. 4 Block diagram of the control architecture on the hexacopter.

Mission Planner with ArduPilot is used as the ground station control software. ArduPilot provides a link between the multirotor and the ground station where telemetry data can be viewed in real time. Using a 915 MHz radio antenna connected to both the multirotor and the ground station computer, the aircraft feeds data on its position and dynamics in real-time to the ground station. The flight controller selects a set of control laws based on its assigned flight mode. During operational and post-rotor failure experiments, the flight controller remained on stabilize mode, requiring that the hexacopter remain straight-and-level when in hover. Contained within the Pixhawk 6C flight controller are two inertial measurement units (IMUs). Both IMUs recorded the multirotor's angular velocities and linear accelerations using a gyroscope and accelerometer. A sample rate of 1 kHz was used by the flight controller to collect data from the IMUs, ensuring that the sampling frequency is above the Nyquist frequency to prevent aliasing of any signals below 500 Hz.

II D. Power Distribution System

Three power distribution circuits used on the hexacopter: a propulsion circuit, control circuit, and rotor shutoff circuit. The propulsion circuit uses a single 4 cell, 5200 mAh discharge, lithium-polymer (LiPo) battery containing 76.96 watt-hours of energy. The propulsion battery connects to a power distribution board which navigates the power to each of the six motors via the ESCs. The control circuit utilizes a 2 cell, 5200 mAh discharge Li-Po battery which connects directly to the flight controller. The flight controller sends power to the accessory control hardware, such as the receiver and GPS. The flight controller, while connected to each of the ESCs, does not distribute the motor's power to the ESCs. This connection purely serves to transmit PWM signals from the flight controller to the ESCs. The shutoff circuit controls the Arduino Due microcontroller and 5V relay that are used to shut off a single rotor. A 1300 mAh discharge, 3 cell Li-Po battery connects to only the Arduino Due microcontroller and provides a total of 12.6V to the microcontroller which gets stepped down to 3.3V. The microcontroller then distributes power to the relay, which accepts 5V to commence activation. All three power distribution systems operate independently of each other, meaning the loss of one system does not affect the ability for either of the other two systems to effectively distribute power. A summary of the three power distribution systems is presented in the block diagram in Fig. 5.

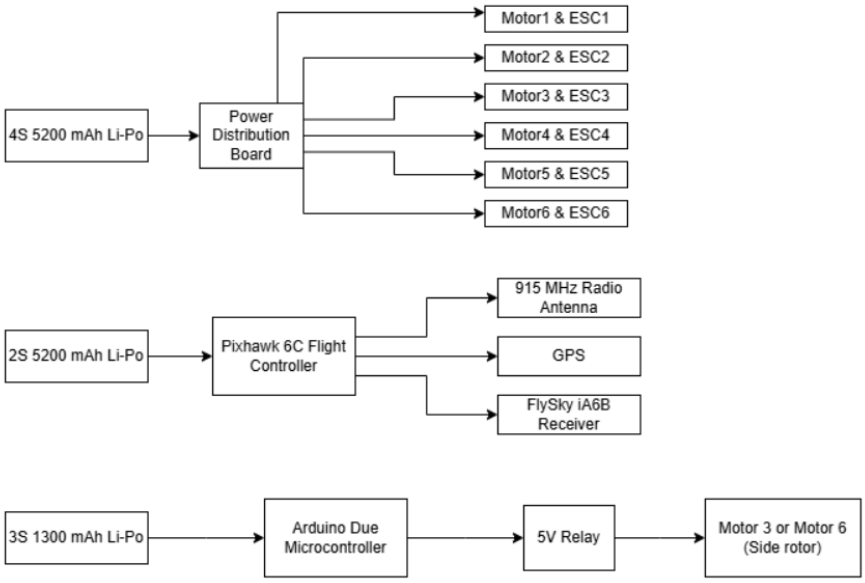

Fig. 5 Block diagram of all three power distribution systems on the hexacopter. Top most diagram is the propulsion circuit, middle diagram is the control circuit, and bottom diagram is the shutoff circuit.

II E. Additional Hardware

Two pieces of additional airborne hardware allow the hexacopter to successfully perform the desired experiments: an Arduino Due microcontroller and a 5V relay. The microcontroller and relay can communicate with each other. Using a script that programs a predetermined delay, the microcontroller switches the relay from the closed to the open position. In operational flight, the microcontroller ensures that the relay holds the "normally closed" position to maintain all six rotors in flight. After the preset 45 second delay, the microcontroller switches the relay to the open position, cutting off power to a single side rotor. The relay accepts 5V power from the Arduino Due microcontroller and is also connected to the microcontroller via the signal pin. On the hexacopter, the relay is spliced between the power distribution board and the ESC of one of the side rotors. The relay receives a signal from the microcontroller to switch off one of the side rotors in order to emulate single-rotor failure. Figure 6 depicts the shutoff circuit placed in the hexacopter in a deconstructed form.

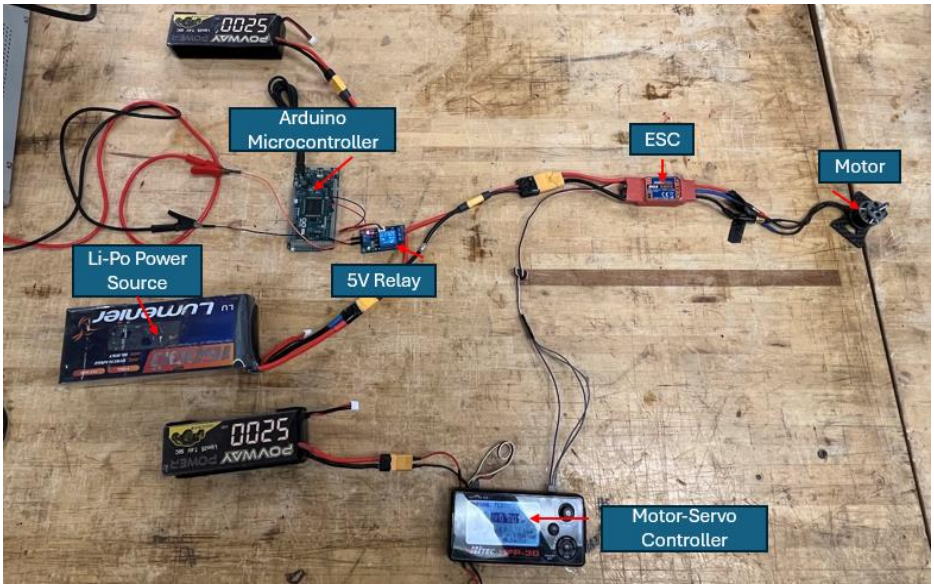

Fig. 6 Deconstructed shutoff circuit. A 5V relay connected to an Arduino Due microcontroller is spliced into the circuit that supplies power to a motor being controlled by an ESC receiving PWM values.

III. Flight Test Methodology

Selecting the correct flying location and weather conditions were important in conducting the flight tests. A flat and open field away from any tall trees was selected to conduct experimental flights. Clear or overcast conditions were present during all flight experiments, and wind conditions were limited to 10 knots or less in any direction. Two open fields created for flying subscale RC aircraft were chosen for their open land free of any tall obstacles. A static calibration was performed before each set of test flights by placing the hexacopter in an equilibrium position after rotating it purely about the pitch and roll axes as suggested by Ref. [5]. In between every trial flight, a simple level calibration was performed on the IMUs (and therefore flight controller) to redefine the level point in case of dislodging of the flight controller after landing.

To evaluate the hexacopter's behavior under operational conditions, the control and propulsion circuits were plugged in, while the shutoff circuit remained unplugged. The ESCs were then armed by the safety pilot to start the motors. The hexacopter was ascended to an altitude of at least 5 feet to avoid ground effects. An altitude of at least 20 feet was preferred to give the multirotor ample airspace to recover from rotor failure. A combination of hover flight and forward flight was performed while the multirotor was in the air for approximately 50 to 60 seconds by the safety pilot. The flight is also filmed from the ground for the entirety of the experiment. Afterwards, the safety pilot brings the multirotor to the ground for landing, and the motors are disarmed. To conduct performance evaluations post-rotor failure, the shutoff circuit was enabled by connecting the power source. The hexacopter was then armed after all six motors were in the operational state, as designated by an audible sound from the motor rearming. Data collection began as soon as the motors were armed. Once armed, the hexacopter was ascended to a hovering state at the aforementioned preferred altitude. After a preprogrammed time delay of 45 seconds after arm, a single side rotor was turned off by the shutoff circuit, and the hexacopter was allowed to recover back into a hovering state. Once its reactionary behavior was measured, the hexacopter was slowly brought down to the ground for a landing and disarmed once it reached the ground.

IV. Data and Results

IV A. Hexacopter Specifications

Parameters regarding the specifications of the hexacopter were determined. These parameters include: weight, max thrust to weight ratio, battery capacity, and center of gravity and are summarized in Table 1. The data collected by the IMU utilizes an axis system and sign convention as follows: the x-axis represents the roll axis forward flight as +x, the y-axis represents the pitch axis with rightward flight as +y, and the z-axis represents the yaw axis with upward flight as +z. Positive roll is a rolling motion towards the right, positive pitch is a downwards pitching motion, and positive yaw is a yawing motion to the right.

Table 1 Summary of hexacopter parameters.

Parameter	Value
Weight (W)	7.20 lb
Thrust (T)	2 lb/motor, 12 lb total
T/W_{amx} (Operational)	1.667
T/W_{max} (Post-Rotor Failure)	1.111 to 1.389
Battery Capacity for Propulsion Rotors	76.96 Wh
C.G. Location (from center of frame)	$0.625\hat{x}$ - $0.1875\hat{y}$ in

IV B. Baseline Performance

Figure 7 shows the raw data recorded by the IMU for the third operational flight that was performed. This data sets a standard for what fully operational flight movement should look like. The third flight was chosen as it provides the most consistent data regarding the hexacopter's dynamics while in the air. The flight data graphed in Fig. 7 spans approximately 100 seconds from takeoff to landing.

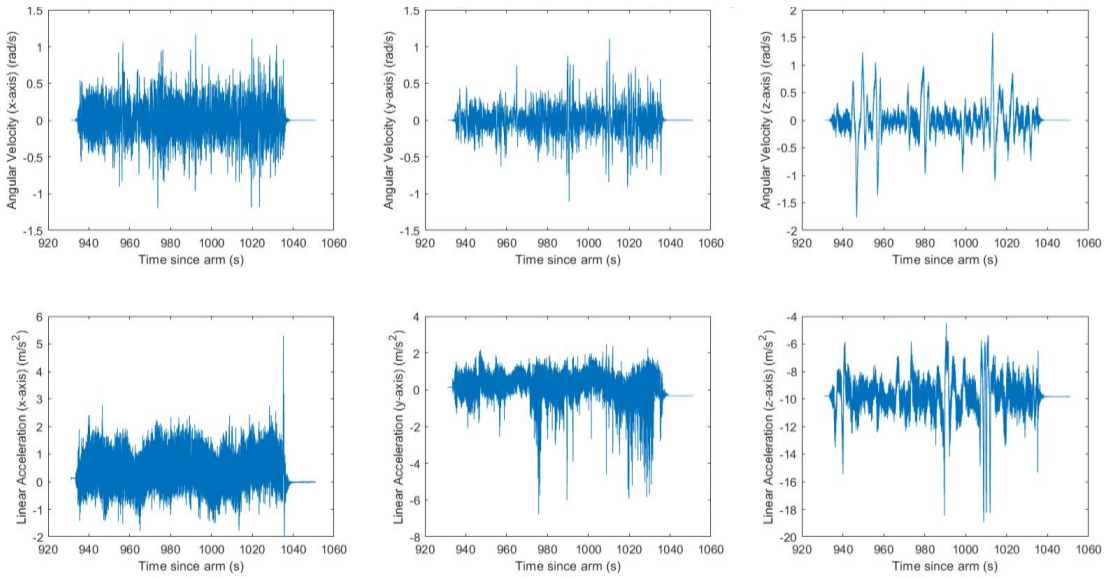

Fig. 7 Raw gyro and accelerometer data from third normal operation flight.

Large spikes in the data may be observed near the end of the recorded data due to the multirotor's movement during landing. The hexacopter tended to not land smoothly and often bounced on landing due to impact with the ground. This could cause some large readings in acceleration and rotational velocity near the end of the recorded data. The z-axis accelerometer reading also records gravity, meaning that the true vertical acceleration must have 9.81 m/s^2 subtracted from the raw data to ensure that acceleration from gravity is accounted for when observing data trends.

Attitude data, as shown in Fig. 8, shows expected results for a normal operations flight. With full control authority, the pitch and roll can be stabilized to 0 radians in hover, while the yaw value is less consequential. The data in Fig. 8 shows no large jumps in pitch and roll, and no unstable yaw motion implying that the hexacopter's motion is fully controllable by the safety pilot.

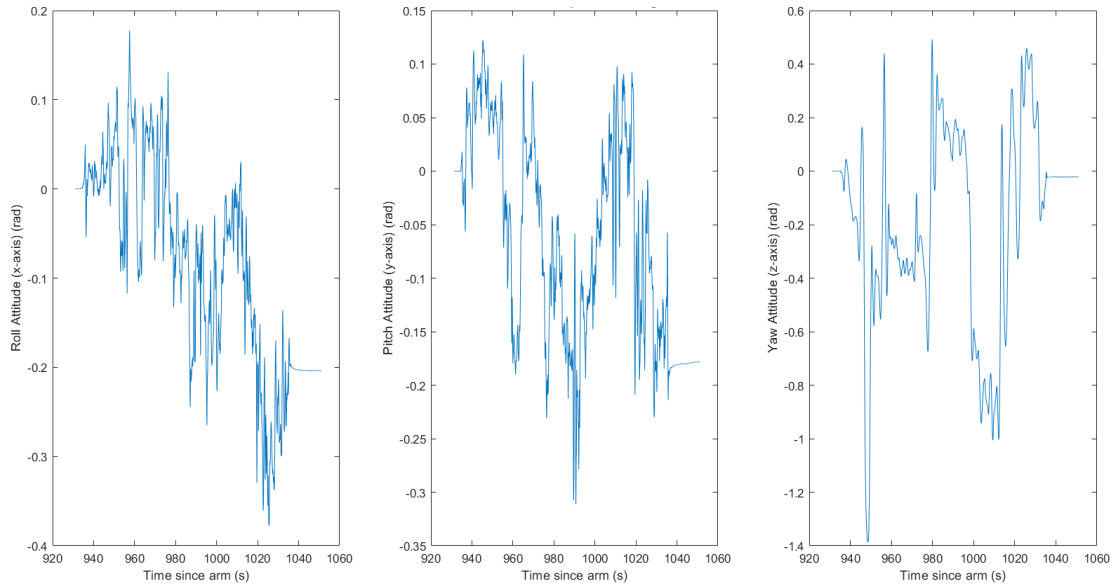

Fig. 8 Attitude data from third normal operation flight.

IV C. Post-Single Rotor Failure Performance

Figures 9 and 10 show the raw gyroscope and accelerometer data as well as the attitude data obtained from integrating the gyroscope's angular velocity data. The raw data shows relatively stable hovering flight until the rotor shuts off occurs roughly 40 seconds after takeoff. After shutoff, the angular velocities and linear accelerations change dramatically before the final spike which occurs during ground impact on landing. Readings before the final spike show a leftward roll, an upward pitch, and a severe counterclockwise yaw from a disabled N-rotor on the left.

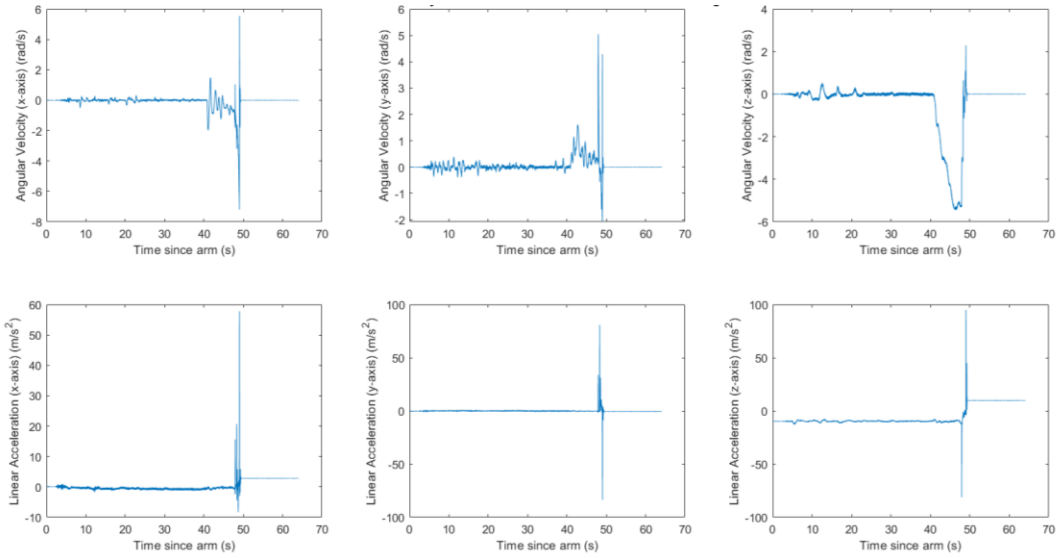

Fig. 9 Raw gyro and accelerometer data from first CCW post-rotor failure flight.

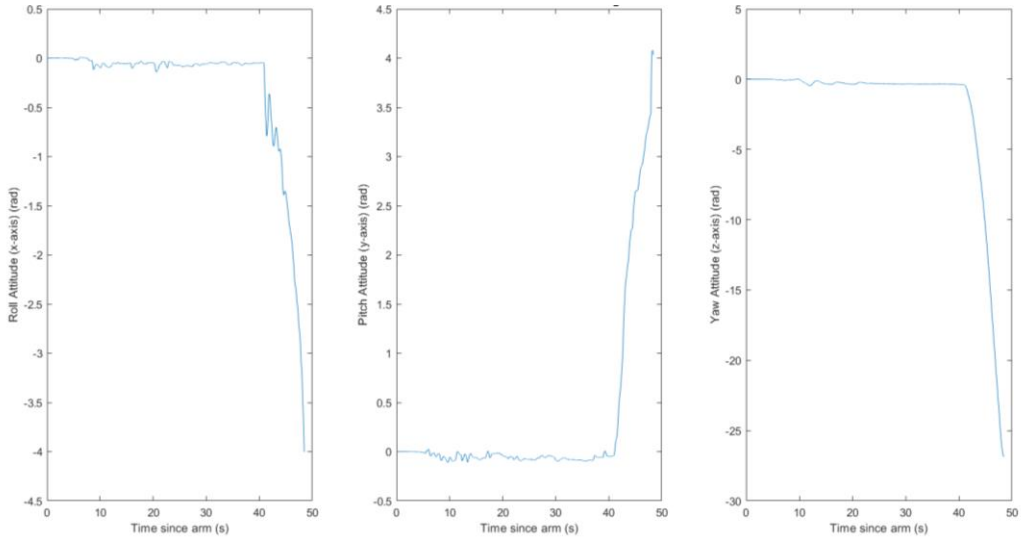

Fig. 10 Attitude data from first CCW post-rotor failure flight.

Similarly, the attitude data derived from the gyroscope readings show a similar story. After rotor failure, the roll and pitch attitude shift to a non-zero value showing that while the flight controller attempts to recover after rotor failure, counterclockwise rotor loss results in an unstable response from the multirotor. Pitch and roll motion from bringing the multirotor to a safe position for landing may have influenced the attitude data. Observations of the hexacopter's movement post-rotor failure line up with the yaw attitude plot, in that the multirotor spun about the yaw axis continuously after losing the counterclockwise rotor. The yaw heading plot shows that the yaw angle increases considerably after rotor failure. It is likely that hysteresis errors occurred in the data collection due to the rapid change in angular velocity during recovery, causing the IMU readings to be offset by a constant amount from the true values.

Hysteresis errors likely contributed to the large drift in the pitch and roll attitudes shown in the plots in Fig. 10 [5]. Figures 11 and 12 show the raw gyroscope and accelerometer data, and the integrated attitude data collected for the first clockwise rotor-failure flight, which was chosen as it was conducted with well-calibrated IMUs. In the raw data in Fig. 11, the motion of the hexacopter post-rotor failure closely resembles the motion during hover, with a large spike at the end due to landing. Angular velocity and linear acceleration values are close to the values seen during operational hovering flight even after rotor loss, with a few of the data such as the linear acceleration in the y-axis having larger amplitudes in the readings.

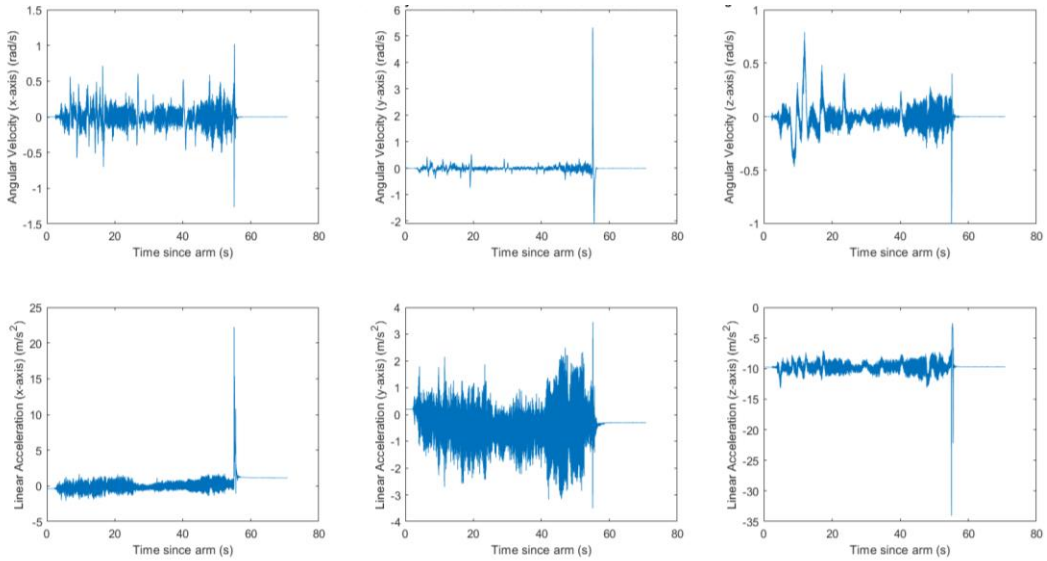

Fig. 11 Raw gyro and accelerometer data from first CW post-rotor failure flight.

Figure 12 shows attitude data that is very similar to that found during hover. After rotor failure, the hexacopter shows a positive roll reaction which very quickly is returned to normal. The multirotor displays no large pitch variation after rotor failure and displays a slight yaw towards the left during its entire flight. Compared to counterclockwise rotor failure, this multirotor, when subject to clockwise rotor failure, is much more stable and has a greater ability to recover from rotor failure and return to a hovering position. Table 2 summarizes the maximum deviation in pitch and roll attitude, as well as the yaw heading angle for the counterclockwise and clockwise rotor failure flight tests.

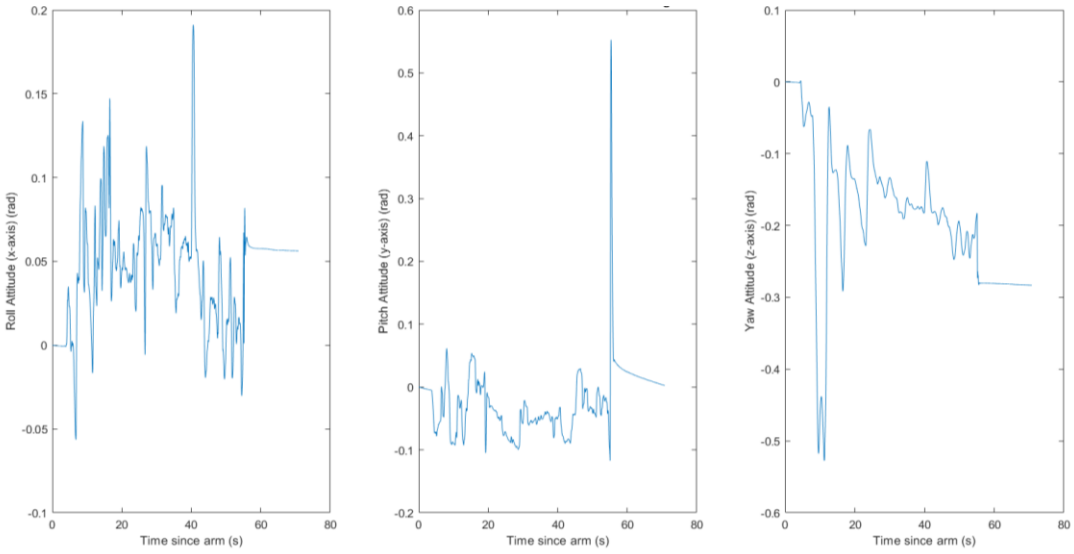

Fig. 12 Attitude data from first CW post-rotor failure flight.

Table 2 Maximum pitch, roll, and yaw deviation post-CCW and post-CW rotor failure.

	θ_{max}	φ_{max}	ψ_{max}
CCW Rotor Failure	-4 rad	4 rad	-26 rad
CW Rotor Failure	0.19 rad	-0.12 rad	-0.53 rad

V. Discussion

V A. Analysis of Control Authority

The data obtained from operational and post-rotor failure demonstrates that counterclockwise rotor-failure resulted in a much more biased response than clockwise rotor failure, which the hexacopter was able to recover from sufficiently. The hexacopter was shown to be able to return to a hovering position after clockwise rotor-failure, but was unable to return to a stable hovering position after counterclockwise rotor-failure, despite the pitch and roll being recoverable. Similar to the behavior described in Ref. [3], a spiraling yawing motion was observed primarily after counterclockwise rotor failure, which suggests the NPNPNP-X hexacopter configuration has a bias for the counterclockwise propellers. A previous evaluation on the ability for a hexacopter to recover from rotor failure lines up with the data obtained in these experiments [4]. Previous observations on single rotor failure of a subscale RC multirotor in an NPNPNP or similar configuration also observed a spiraling yawing motion from the hexacopter after counterclockwise rotor failure, but not after clockwise rotor failure [4]. Results from the empirical evaluation qualitatively align with the findings in Ref. [7], in that loss of a single rotor was recoverable but lacked control authority post-recovery. The available control authority index as defined in Ref. [8] (ACAI) of different multirotor configurations found that the PNPNPN-+ configuration operated under an ACAI of 1.4861 during normal operational flight. However, after a single-rotor failure, this ACAI value was reduced to 0, rendering the multirotor uncontrollable, though still able to maintain a hovering position. The PNPNPN-+ configuration is similar to the NPNPNP-X configuration used in the empirical evaluation conducted, in that rotors alternate between clockwise and counterclockwise spin in order to counteract each rotor's torque, resulting in similar behavior between the two configurations [8].

Table 3 ACAI values for operational and post-single rotor failure flight of a PNPNPN hexacopter.

Rotor Failure	ACAI	Controllability
No failure	1.4861	Controllable
$f_1 = 0$	0	Uncontrollable
$f_2 = 0$	0	Uncontrollable
$f_3 = 0$	0	Uncontrollable
$f_4 = 0$	0	Uncontrollable
$f_5 = 0$	0	Uncontrollable
$f_6 = 0$	0	Uncontrollable

Source: Du, Quan, Yang, & Cai. [8]

V B. Challenges and Limitations

The T/W of the multirotor used in these experiments also displays some of the challenges in having sufficient recovery ability post-rotor failure. Under operational flight, the T/W of the multirotor was 1.67 compared to the T/W after a single rotor failure of 1.39. If swapped to a quadcopter configuration, the multirotor would have had a T/W of only 1.11. To hover sufficiently, the multirotor must have a T/W of at least 1, whereas a recommended T/W for the hexacopter to perform effective recovery would be closer to 2. The hexacopter built for these empirical evaluations lacked a sufficient T/W for an optimal recovery and may have suffered a larger attitude loss than if a different

configuration was used. NPNPNP or PNPNPN are also not the only functional configurations for a hexacopter. Other configurations include a PPNNPN-+ configuration or a NPPPNN-X configuration [4]. Observing the yaw bias that occurred during CCW rotor shutoff, NPNPNP may not be the optimal configuration for control authority in the event of rotor failure. Other hexacopter configurations may allow for more stable correction depending on how the rotor spin directions are placed along the frame.

VI. Conclusion

Experimental empirical evaluations were conducted on a subscale hexacopter to evaluate the response, recovery, and performance to single rotor failure. Counterclockwise side rotor loss was shown to be much more dramatic and harmful to the controllability of the hexacopter than clockwise rotor loss due to the spiraling yaw motion from the yaw bias that occurs after counterclockwise rotor failure confirmed by observations in Ref. [4]. The NPNPNP-X configuration hexacopter loses its control authority after a single rotor failure, as its ACAI value falls from 1.4861 to 0 if any of the six rotors fails in flight [8]. Thus, after losing control, the hexacopter only can correct back into a stable hovering position but does not have the authority to be controlled by on-board systems or a safety pilot. The NPNPNP hexacopter configuration is shown to be largely unstable when subjected to rotor failure and requires incredible precision to recover and maintain hovering flight after rotor failure [8]. NPNPNP configurations may operate in a more stable manner post-rotor failure if the hexacopter adapts an NPNP quadcopter configuration afterwards, although this leads to a lack of control authority as adjacent rotors no longer have opposite rotations [7]. The loss of forward and aft rotors can also be evaluated through an empirical study and compared to simulation results such as those presented in Ref. [7]. Future experiments involving larger scale multirotors and other hexacopter configurations can be conducted to determine the configuration that provides the most control authority post-rotor failure. By scaling up the size of the experimental hexacopter, the behavior of the aircraft will more closely match the behavior of a full-scale urban air mobility (UAM) hexacopter, allowing for the results of the experiment to be scaled and generalized to UAM aircraft.

Acknowledgments

The authors thank North Carolina Space Grant for providing the undergraduate research scholarship award which makes this project possible. Along with assistance from Leo Bergmann, James Sorber, and Max Shipp from the Aerial Robotics Club at NC State (ARC) for their contributions to test flights and assistance with microcontrollers. As well as Nicholas Garcia and Ben Kreager from the Micro/Nano Engineering Lab (MNEL) at NC State for support on relays and research advice.

References

[1] Silva, C., Johnson, W., Antcliff, K. R., & Patterson, M. D., 'VTOL Urban Air Mobility Concept Vehicles for Technology Development', *2018 Aviation Technology, Integration, and Operations Conference*, 2018. pp. 2-16.
doi: 10.2514/6.2018-3847
[2] Bahr, M., McKay, M., Niemiec, R., and Gandhi, F., 'Post-Motor-Failure Performance of a Robust Feedback Controller for a UAM-Scale Hexacopter', *Proceedings of the 77th Vertical Flight Society Annual Forum*, 2021.
doi: 10.4050/F-0077-2021-16783
[3] Scaramuzza D, Achtelik M, Doitsidis L, et al., 'Vision-controlled micro flying robots: from system design to autonomous navigation and mapping in GPS-denied environments', *IEEE Robotics & Automation Magazine*, Vol. 21, 2014. p. 4.
doi: 10.1109/MRA.2014.2322295
[4] Oliver, J., 'Hexacopter and motor loss | ArduPilot' Available: https://discuss.ardupilot.org/t/hexacopter-and-motor-loss/57942
[5] Shi, Dongjie & Yang, Binxian & Quan, Quan. 'Reliability analysis of multicopter configurations based on controllability theory', *Proceedings of the 35th Chinese Control Conference*, 2016. P.6744
doi: 10.1109/ChiCC.2016.7554418
[6] Wheeler, A. J. & Ganji, A. R., 'Introduction to Engineering Experimentation: Third Edition', 2010. pp. 13-28.
[7] McKay, M., Niemiec, R., & Gandhi, F., 'Control Reconfiguration for a Hexacopter Experiencing Single Rotor Failure', *27 th International Conference on Adaptive Structures and Technologies*, 2016. p. 3-6
doi:
[8] Du, Guang-Xun & Quan, Quan & Yang, Binxian & Cai, Kai-Yuan. 'Controllability Analysis for Multirotor Helicopter Rotor Degradation and Failure', *Journal of Guidance Control and Dynamics*, 38. 2015. p. 981.
doi: 10.2514/1.G000731